Sarcoidosis of the CNS: Comparison of Unenhanced and Enhanced MR Images

John L. Sherman[1,2]
Barney J. Stern[3]

Sarcoidosis involving the CNS has a predilection for the leptomeninges, although parenchymal involvement occurs. We retrospectively evaluated the appearance of CNS sarcoidosis on unenhanced and enhanced MR images. MR studies were abnormal in 17 of 20 patients with CNS sarcoidosis. In all 17 patients, meningeal disease was detected on the gadopentetate-dimeglumine–enhanced T1-weighted images; the disease was detected on unenhanced images in three patients. Well-defined leptomeningeal patterns of enhancement were present in 15 patients. Other areas of involvement were the dura; brain parenchyma including hypothalamus, periventricular white matter, and ventricular ependyma; optic chiasm; and pituitary gland.

Gadopentetate dimeglumine optimally evaluates meningeal disease and highlights the importance of the leptomeninges and Virchow-Robin spaces in the pathogenesis of CNS sarcoidosis. Enhanced MR is the preferred imaging technique for the evaluation of CNS sarcoidosis.

***AJNR* 11:915–923, September/October 1990; *AJR* 155: December 1990**

Neurologic manifestations of sarcoidosis occur in 5% of patients with this disease [1]. Postmortem studies demonstrate CNS and meningeal disease in as many as 14% of patients with known systemic sarcoidosis [2, 3]. Intracranial involvement is most often a diffuse or focal granulomatous leptomeningitis. Parenchymal inflammation is seen also. The MR appearance of neurosarcoidosis has been described [4–8]. Unenhanced MR is superior to CT in the evaluation of hypothalamic and periventricular involvement [3, 4]. However, unenhanced MR does not optimally evaluate inflammation of the meninges and does not evaluate the integrity of the blood-brain barrier. The use of gadopentetate dimeglumine has been recommended for brain MR imaging to evaluate the blood-brain barrier and whenever extraaxial disease is suspected [9–13]. In this study, we describe the gadopentetate-dimeglumine–enhanced MR appearance of CNS sarcoidosis and compare it with the unenhanced MR appearance.

Materials and Methods

Twenty patients with neurosarcoidosis underwent MR examinations of the brain before and after administration of gadopentetate dimeglumine. All but three patients had biopsy-proved systemic sarcoidosis. In those three patients, intracranial biopsies showed granulomatous inflammation consistent with sarcoidosis. The diagnosis of neurosarcoidosis was made clinically in the other 17 patients. There were 11 women and nine men 21–58 years old (average, 36 years). Table 1 is a clinical summary of the patients involved in this study.

MR examinations were performed on 1.5-T (n = 16 patients), 1.0-T (n = 1 patient), or 0.5-T (n = 3 patients) MR imagers. All unenhanced examinations used at least three techniques: T1-weighted spin echo (SE), 500–600/20–25/2 (TR/TE/excitations); intermediate SE, 2000–3200/30–40/1–2; and T2-weighted SE, 2200–3200/80–100/1–2. Section thickness was 5 or 7 mm, with an intersection gap of 1–2.5 mm. Gadopentetate dimeglumine (Magnevist, Berlex

Received December 6, 1989; revision requested February 15, 1990; revision received March 27, 1990; accepted March 29, 1990.

[1] Washington Imaging Center, 2801 University Blvd., Kensington, MD 20895. Address reprint requests to J. L. Sherman.

[2] Department of Radiology, Uniformed Services University of the Health Sciences, Bethesda, MD 20814, and George Washington University School of Medicine, Washington, DC 20037.

[3] Division of Neurology, Sinai Hospital of Baltimore, Baltimore, MD 21215, and Department of Neurology, The Johns Hopkins Medical Institutions, Baltimore, MD 21205.

0195-6108/90/1105-0915
© American Society of Neuroradiology

TABLE 1: Clinical Summary of Patients with CNS Sarcoidosis

Case No.	Age (yr)	Race	Sex	Neurologic Signs and Symptoms	Tissue Diagnosis	Systemic Disease	Steroid Therapy at Time of MR
1	34	B	F	Neuroendocrinologic dysfunction	Lung	Yes	Yes
2	49	B	M	Encephalopathy, ataxia	Brain	Yes	No
3	23	B	F	Papilledema, aseptic meningitis	Lung	Yes	No
4	34	B	F	Neuroendocrinologic dysfunction, aseptic meningitis	Nasal	Yes	No
5	21	B	M	Seizures, cranial nerve II	Node	Yes	Yes
6	27	B	M	Seizures, cranial nerves I, II, VIII	Node	Yes	No
7	58	W	F	Hypothalamic dysfunction, encephalopathy, cranial nerves I & II	Sinus	Yes	No
8	31	B	M	Hypothalamic dysfunction, cerebellar signs, ataxia	Testis	Yes	No
9	48	W	M	Seizures, encephalopathy, cranial nerves II & VIII	Brain	No	Yes
10	38	B	F	Neuroendocrinologic dysfunction	Lung	Yes	No
11	57	B	M	Cranial nerves II & VIII	Lung	Yes	No
12	39	W	M	Hemiparesis, cranial nerve II	Conjunctival	Yes	No
13	29	B	M	Papilledema, headache, cranial nerve I	Brain	No	Yes
14	31	B	F	Cranial nerves VII & VIII	Lung	Yes	No
15	40	B	F	Cranial nerves V & VIII	Node	Yes	No
16	30	B	F	Aseptic meningitis, cranial nerve VIII	Liver	Yes	No
17	32	B	F	Seizures, cranial nerves II & VIII; hypothalamic dysfunction	Brain	No	Yes
18	32	B	F	Seizures, cranial nerves I, II, & VIII; pituitary dysfunction	Brain	Yes	No
19	36	B	F	Encephalopathy, dysarthria pituitary dysfunction	Lymph node	Yes	No
20	29	B	M	Cerebellar signs, ataxia, encephalopathy	Lung	Yes	No

Laboratories, Wayne, NJ) was given in a concentration of 0.1–0.15 mmol/kg at a rate of 15–30 ml/min (Kashanian FK et al., presented at the annual meeting of the American Society of Neuroradiology March 1989). Patients were studied with short T1-weighted scans after the administration of contrast material. The matrix was 256 × 256 for all T1-weighted images and for most intermediate and T2-weighted images. A 128 × 256 matrix was used in a few instances.

In a nonblinded review, we retrospectively analyzed each set of images for abnormalities affecting the following areas: meninges, falx, hypothalamus/pituitary, periventricular white matter, parenchyma, and ependyma.

Results

The results of brain MR in our patients are summarized in Table 2. The enhanced MR studies revealed additional areas of involvement not suspected on the unenhanced examinations in 17 patients. We identified multiple lesions in most patients; for example, multiple meningeal foci, hypothalamic infiltration, and white or gray matter lesions. The scope and multiplicity of the variable MR findings on CNS sarcoid in our patients is reflected in Table 3. Of particular note is the observation of multiple areas of involvement that were visualized only on enhanced MR. Leptomeningeal involvement (Figs. 1–5) was most striking since none of the leptomeningeal disease was detected on unenhanced MR. Of interest is the observation of internal auditory canal enhancement in three patients with diffuse leptomeningeal disease. Other areas where enhanced MR was superior included the dura (Figs. 1 and 5), hypothalamus, and pituitary/infundibular disease (Figs. 1, 3, and 6). Periventricular enhancement (Figs. 6 and 7) was very prominent in several patients and could not be predicted on the basis of the appearance on the T2-weighted images.

Clinical Correlation and Follow-up Evaluation

The clinical summary of our patients is presented in Table 1. Three patients had a clinical diagnosis of CNS sarcoidosis with cranial neuropathies but had normal MR studies. Two of these patients were being treated with 40 mg/day of prednisone at the time of scanning.

Follow-up gadopentetate-dimeglumine–enhanced MR studies were available in four patients. Three of the patients were treated with 20–65 mg/day of prednisone. In one patient (case 13), a right cerebellopontine angle granuloma markedly decreased in size after 2 months of therapy but then stabilized over the next 12 months. A second patient (case 7, Fig. 6) had resolution of abnormal enhancement around the third ventricle but persistent chiasmatic enhancement after 6 months of corticosteroid therapy (40 mg of prednisone/day tapered to 10 mg/day). In a third patient (case 4), an unenhanced study initially revealed brain edema adjacent to an area of slight falcine thickening. Follow-up unenhanced and

TABLE 2: Summary of Brain MR Imaging in Patients with CNS Sarcoidosis

Case No.	Meningeal Disease		Hypothalamus and Pituitary	Periventricular White Matter Lesions	Ependymal Enhancement	Parenchymal Involvement	Hydrocephalus
	Leptomeningeal	Dural					
1	Diffuse (G)	None	G	U	No	None	No
2	Diffuse (G)	None	None	G/U	No	Edema, encephalopathy, meningovasculopathy (G/U)	No
3	Diffuse (G)	None	G/U	None	No	None	No
4	Diffuse (G)	None	G/U	None	No	Edema (U)	No
5	Diffuse (G)	G	G/U	G/U	No	Edema, encephalopathy (G/U)	No
6	Diffuse (G)	G/U	None	None	No	Two parenchymal nodules without surrounding edema (G)	No
7	Focal (G)	None	G	G/U	No	No	Yes
8	Focal (G)	None	None	None	Yes	Cerebellar peduncle infarct (U)	Yes
9	Focal (G)	None	None	U	No	None	Shunted
10	Focal (G)	None	G/U	G	No	None	No
11	Focal (G)	None	None	G/U	No	Enhancing cerebellar peduncle and posterior temporal lesions (G/U)	No
12	None	G	G	None	No	Internal capsule lacune (U)	No
13	None	G/U	None	None	No	None	Shunted
14	None	None	None	None	No	None	No
15	None	None	None	None	No	None	No
16	None	None	None	None	No	None	No
17	Diffuse (G)	None	G	G/U	No	Edema, confluent nodules causing mass in temporal lobe (G/U)	No
18	Diffuse (G)	G/U	G/U	None	No	Edema, encephalopathy (G/U)	No
19	Diffuse (G)	None	G	None	Yes	None	Yes
20	Diffuse (G)	G	None	None	No	Edema, subfrontal mass extending into frontal lobe (G/U)	No

Note.—G = enhancing abnormality identified on gadopentetate-dimeglumine–enhanced MR; U = abnormality identified on unenhanced MR.

TABLE 3: Summary of MR Characteristics of CNS Sarcoidosis

Involved Area	T2-Weighted Images	T1-Weighted Images	T1-Weighted Images with Gadopentetate Dimeglumine
Leptomeninges	No lesions detected	No lesions detected	Diffuse involvement (n = 10); focal involvement (n = 5)
Dura	Hypointense plaque (n = 3); isointense mass (n = 1) [4]	Isointense mass (n = 1)	Focal mass/plaque (n = 3); sheetlike involvement (n = 3) [13]
Pituitary and infundibulum	No lesions detected	Isointense enlargement (n = 5)	Increased enhancement of infundibulum (n = 5) and pituitary (n = 1)
Optic chiasm	No lesions detected	Enlarged chiasm (n = 5) [4]	Enhancement of chiasm (n = 6) and optic nerves/tracts (n = 2)
Hypothalamus	Hyperintensity in anterior perforated substance (n = 4) and anterior commissure (n = 2) [14]	No lesions detected	Enhancement of hypothalamic area (n = 4) and fornix (n = 2)
White matter	Vasogenic edema (n = 6); patchy periventricular/subcortical lesions (n = 6) [4, 6, 8]	No lesions detected	Enhancement near lateral ventricles (n = 3), near third ventricle (n = 3), and near fourth ventricle (n = 3)
Gray matter	Heterogeneous infiltrations with edema (n = 5) and without edema (n = 1) [4, 6, 7]	Hypointense area (n = 2)	Small discrete nodules (n = 5); linear/confluent nodular areas in continuity with pial disease (n = 4)
Ventricles	Hydrocephalus with periventricular edema (n = 3); "ballooning" of fourth ventricle (n = 1)	Hydrocephalus (n = 3) [4, 6]	Periaqueductal enhancement (n = 2); fourth ventricle enhancement (n = 4)

Note.—There was more than one area of involvement in most patients. Cited literature illustrates characteristics of CNS sarcoid.

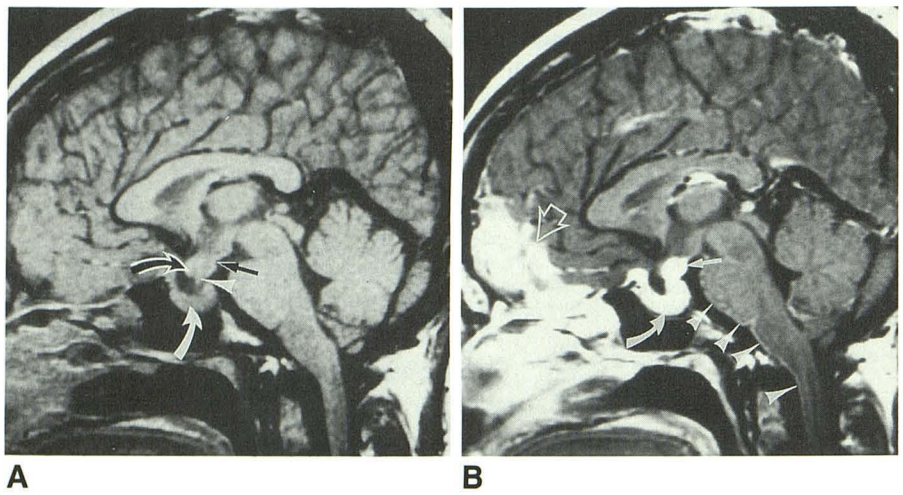

Fig. 1.—Case 4: 34-year-old woman with CNS sarcoidosis involving meninges, pituitary, and hypothalamus.

A, Unenhanced T1-weighted midsagittal image. Pituitary (*white arrow*), infundibulum (*arrowhead*), tuber cinereum (*straight arrow*), and chiasm (*curved black arrow*) are enlarged.

B, Contrast-enhanced T1-weighted midsagittal image shows extensive enhancement of falx and subfrontal meninges (*open arrow*). Note sharply demarcated enhancement of brainstem pia mater (*arrowheads*). Pituitary enhances intensely and is enlarged (*white arrow*). Enhancing pituitary infundibulum, tuber cinereum, and chiasm cannot be differentiated on enhanced image (*straight solid arrow*).

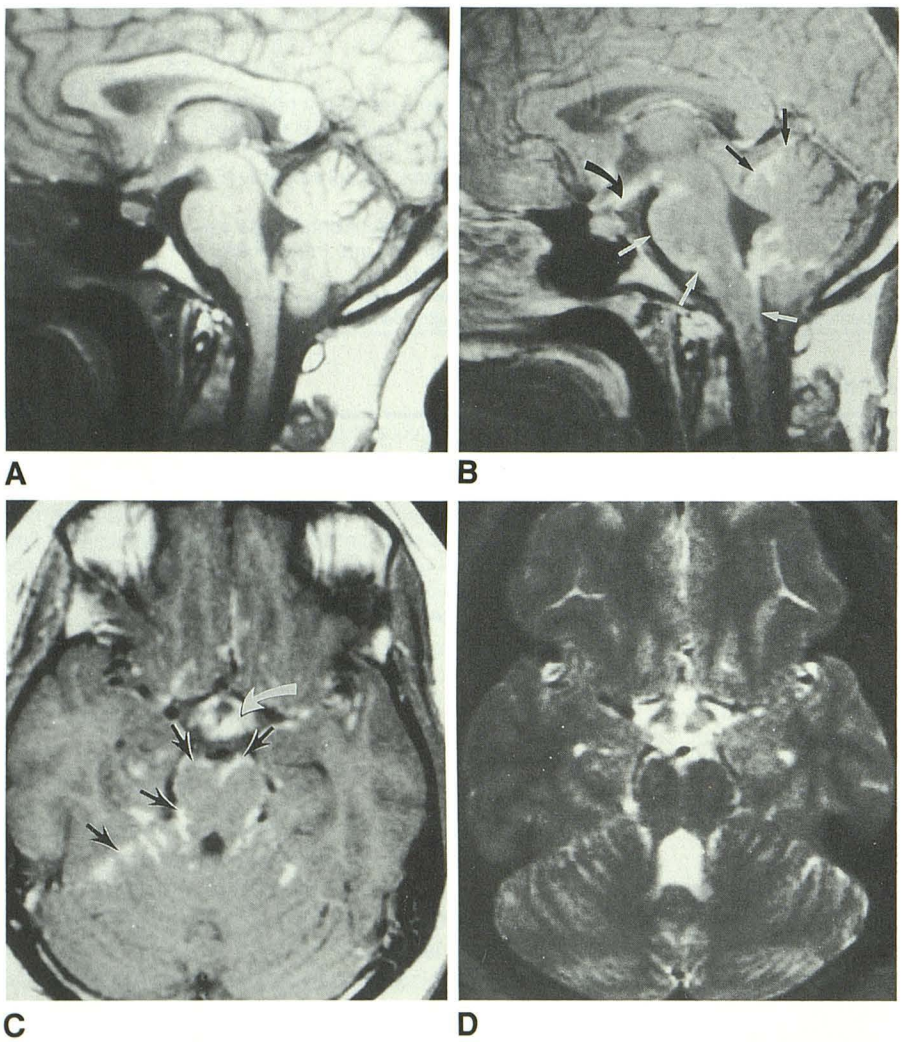

Fig. 2.—Case 1: 34-year-old woman with CNS leptomeningeal sarcoid.

A, Normal unenhanced T1-weighted midsagittal image.

B, Contrast-enhanced T1-weighted midsagittal image shows diffuse leptomeningeal enhancement. Note enhancement of chiasm (*curved arrow*), cerebellum, tectum, and margin of brainstem (*straight arrows*).

C, Enhanced T1-weighted axial image. Enhancement around midbrain and cerebellar hemisphere (*straight arrows*) indicates breakdown of blood-CSF barrier. Optic chiasm involvement (*curved arrow*).

D, T2-weighted image at same level shows no evidence of abnormal signal in brainstem. CSF-brain barrier is probably intact.

enhanced studies 10 months later revealed marked multifocal meningeal and hypothalamic enhancement (Fig. 1), but the brain edema had resolved without corticosteroid administration. The fourth patient (case 5), with extensive meningeal and hypothalamic involvement, was evaluated after 6 months and again after 10 months of suboptimal therapy (80 mg/day of prednisone was prescribed but the patient repeatedly missed doses). Brain edema initially improved but then remained unchanged. Extensive meningeal and parenchymal enhancement was present on the latest contrast-enhanced

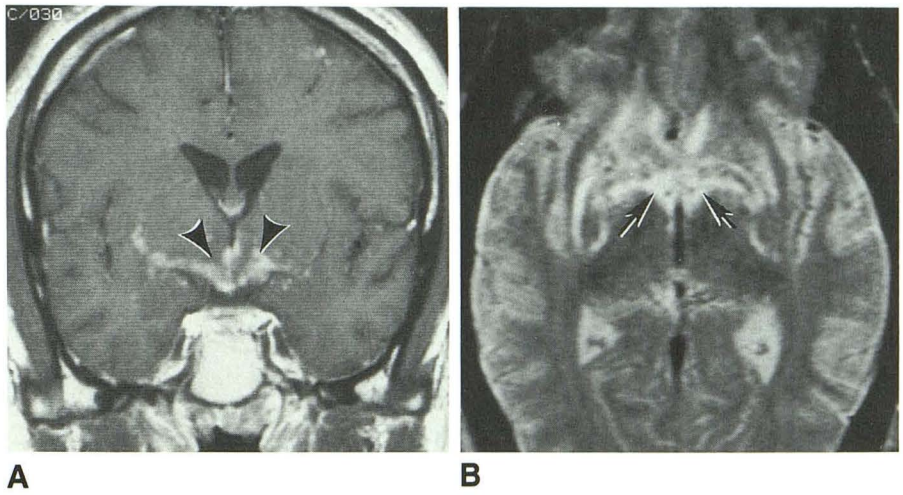

Fig. 3.—Case 5: 21-year-old man with leptomeningeal and hypothalamic involvement.

***A*, Coronal enhanced T1-weighted image. Note basilar leptomeningeal enhancement. Disease extends through anterior perforated substance into hypothalamus (*arrowheads*).**

***B*, T2-weighted axial image reveals edema in base of brain (*arrows*).**

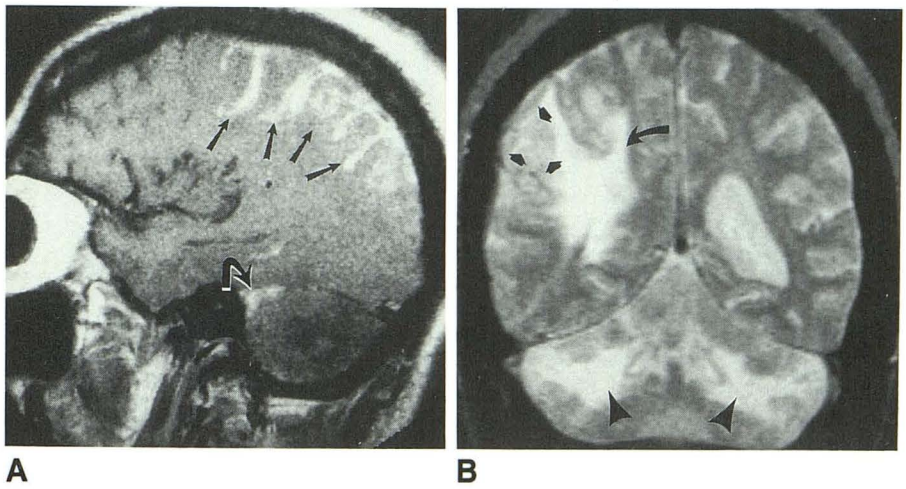

Fig. 4.—Case 2: 49-year-old man with meningoencephalovasculopathy.

***A*, Contrast-enhanced T1-weighted parasagittal image. Note extension of granulomatous disease deep into brain along Virchow-Robin spaces (*straight arrows*). Small area of enhancement (*curved arrow*) and large areas of hypointensity are noted in cerebellum.**

***B*, T2-weighted coronal image. Cerebral cortical disease (*straight arrows*) and vasogenic edema (*curved arrow*). Cerebellar hyperintensity is not associated with mass effect and probably reflects chronic ischemic disease (*arrowheads*).**

MR study (Fig. 3). Visual symptoms had increased. In case 17, CNS involvement increased despite chemotherapy with a regimen of prednisone (15 mg/day) and cyclosporine (trough blood level of 228 ng/ml).

Discussion

Our data concur with pathologic studies of CNS sarcoidosis that have shown that the most common sites of disease activity are the basal meninges; basal midline structures, especially hypothalamus; infundibulum; pituitary gland; and floor of the third ventricle [1, 14]. The pathologic manifestations of CNS sarcoidosis consist of granulomatous dural invasion with plaquelike or focal masses [4, 15], leptomeningitis, parenchymatous infiltration especially along the perivascular spaces of Virchow-Robin [16], and coalescence of granulomata in the brain parenchyma producing an intraaxial tumor [17]. Periventricular lesions in CNS sarcoidosis have been described also [1, 5, 8, 18].

Prior to the release of gadopentetate dimeglumine, our recommendation had been to perform both MR and contrast-enhanced CT [4]. Contrast-enhanced CT was most valuable in the detection of basal meningeal disease, while conventional unenhanced MR revealed involvement of the hypothalamus, optic chiasm, and brain parenchyma including periventricular white matter disease. However, this combined technique is still inadequate for evaluation of the meninges. Contrast-enhanced CT is suboptimal because of the Hounsfield artifact problem [13]. Unenhanced MR is suboptimal because of the poor contrast between bone, CSF, and meninges on both T1- and T2-weighted sequences.

The introduction of gadopentetate dimeglumine markedly increased the sensitivity of MR to the presence of meningeal disease [12]. We detected meningeal disease on the enhanced MR images in 17 patients, compared with unenhanced MR detection in three patients.

Sarcoidosis primarily involves the leptomeninges, which include both arachnoid and pia mater. The leptomeningeal pattern is recognized on enhanced MR images because the enhancement follows the contour of the brain, extending into the cortical sulci. Pial involvement can be differentiated from arachnoid involvement along the brainstem, where the arachnoid is separated from the pia by CSF in the cisternal subarachnoid space (Fig. 1). Here the pia mater is attached

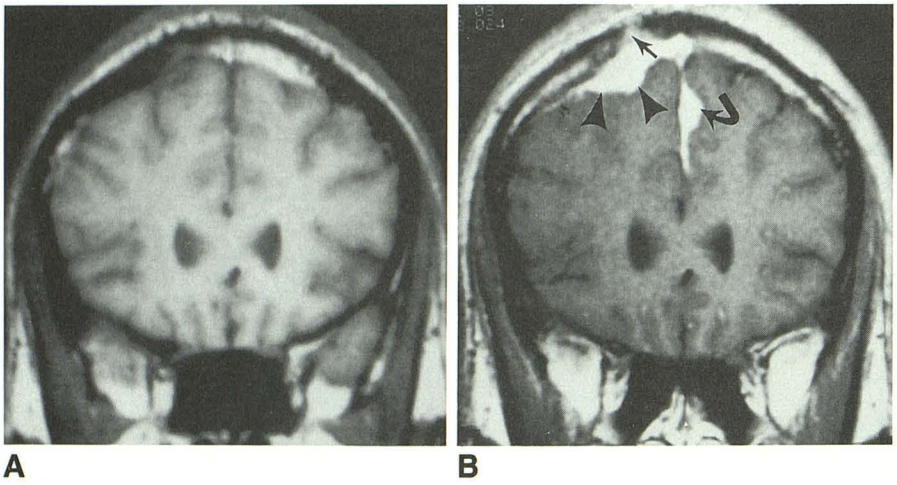

Fig. 5.—Case 6: 27-year-old man with dural, leptomeningeal, and parenchymal disease.

A, Unenhanced T1-weighted coronal image reveals subtle abnormalities that are detectable when compared with enhanced image (*B*).

B, Contrast-enhanced T1-weighted coronal image. Nodular enhancing sarcoid granulomatous mass is on right (*arrowheads*). There is erosion of inner table of calvaria (*straight arrow*). Falx is involved also (*curved arrow*).

C, Contrast-enhanced T1-weighted axial image. Subtle leptomeningeal enhancement is noted in many sulci. Cortical nodule in left temporal lobe was seen only on enhanced image (*arrows*).

D, T2-weighted axial image at same level is normal.

E, T2-weighted axial image near convexity. Brain edema is present (*arrows*).

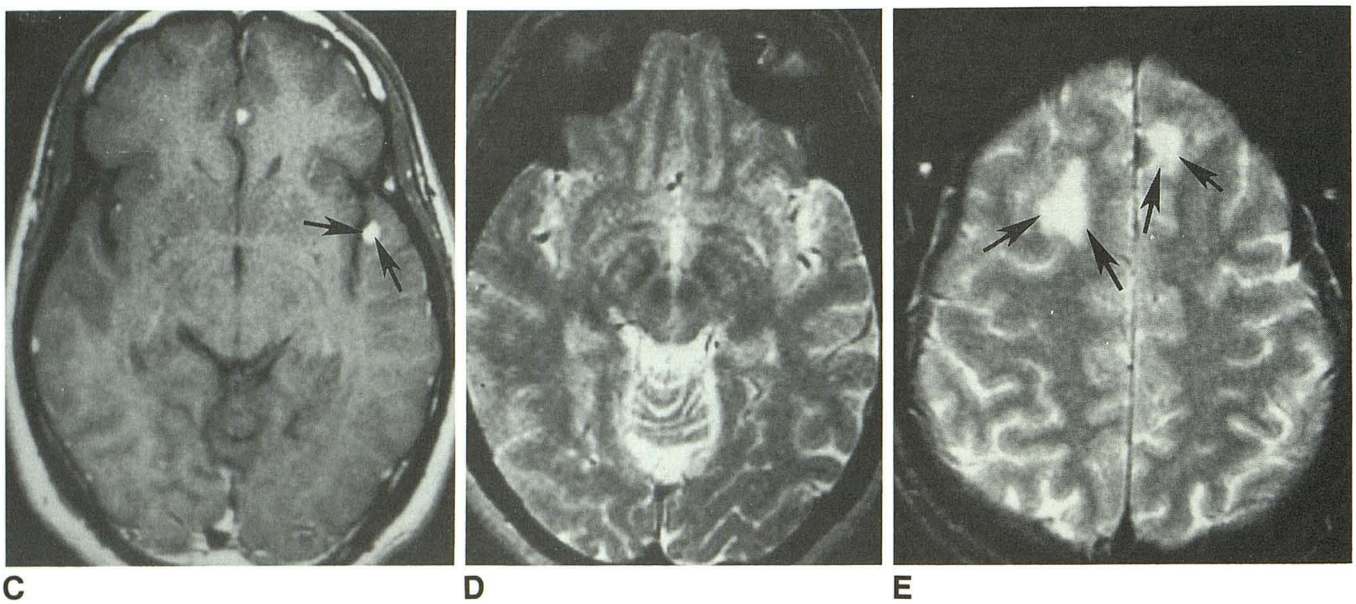

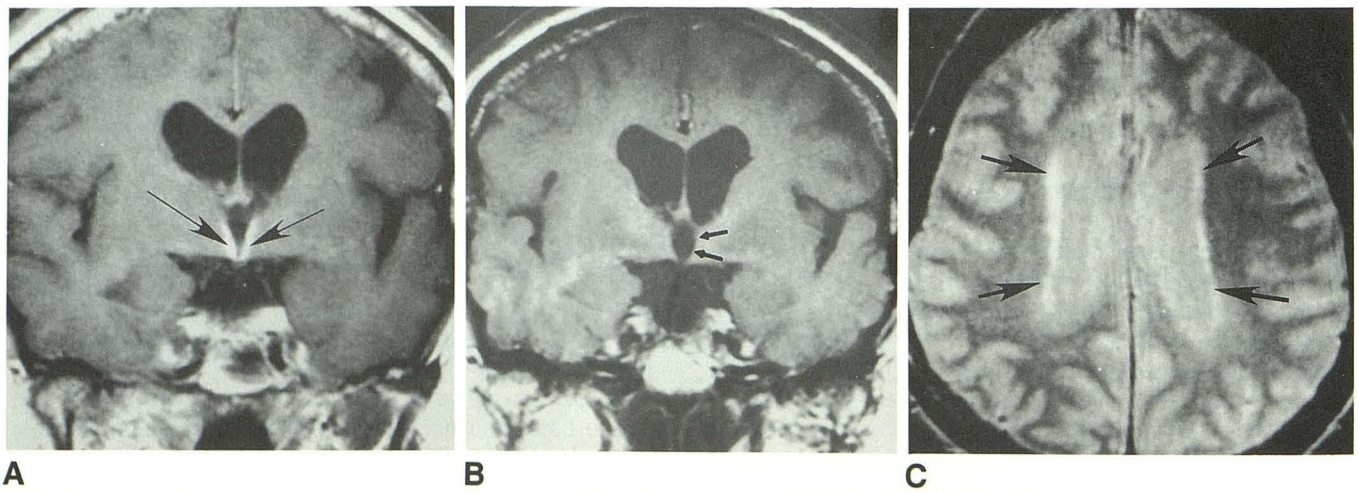

Fig. 6.—Case 7: 58-year-old woman with periventricular and hypothalamic disease.

A, Contrast-enhanced T1-weighted coronal image. Enhancing tissue along margin of third ventricle (*arrows*) causes slight compression of ventricle.

B, Contrast-enhanced T1-weighted image after 6 months of prednisone therapy. There has been resolution of enhancement and relief of mass effect (*arrows*). Note rounded appearance of third ventricle compared with *A*.

C, T2-weighted axial image (pretreatment). Note periventricular areas of increased intensity (*arrows*).

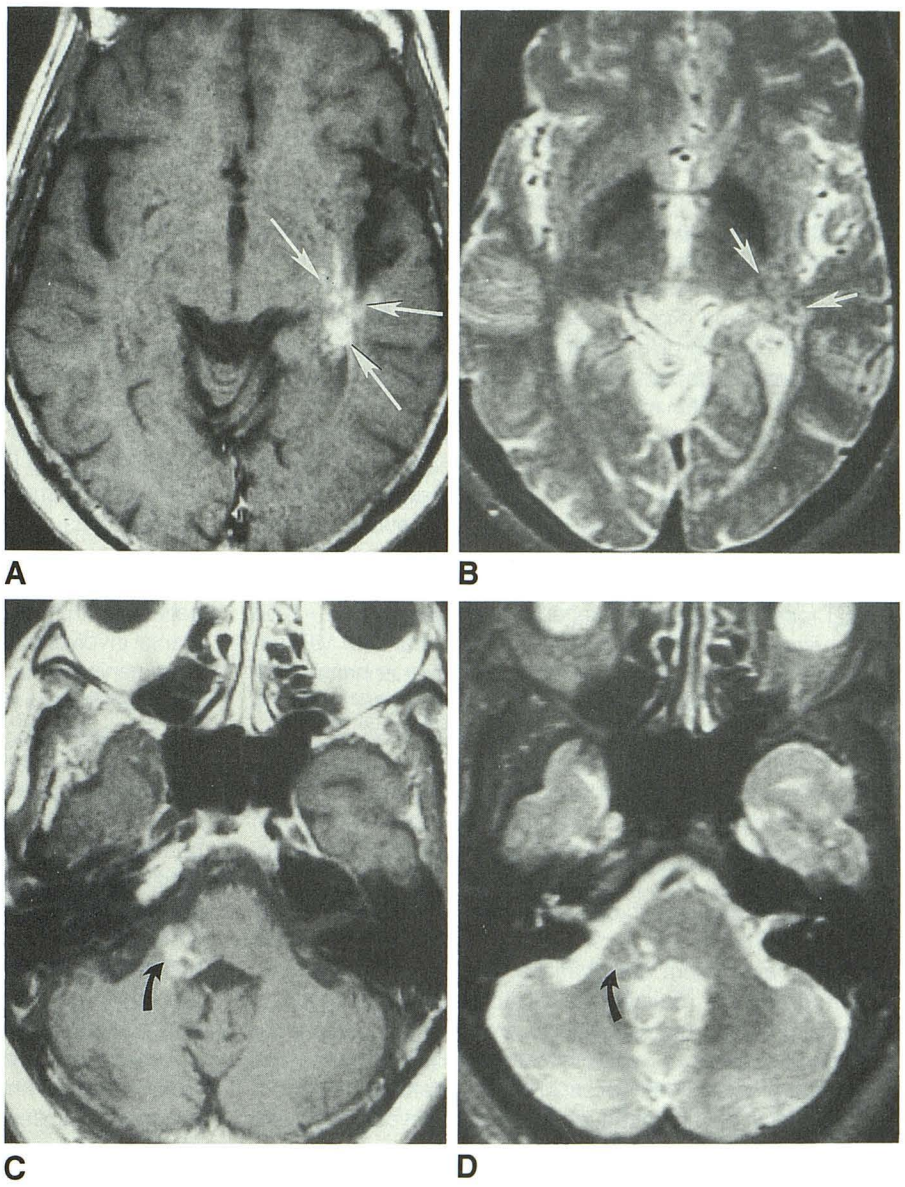

Fig. 7.—Case 11: 57-year-old man with parenchymal disease.

***A*, Contrast-enhanced T1-weighted axial image. Enhancing lesion involves subcortical and periventricular areas (*arrows*).**

***B*, T2-weighted axial image. Small areas of increased intensity are present but there is no evidence of vasogenic edema (*arrows*).**

***C*, Contrast-enhanced T1-weighted axial image in posterior fossa shows enhancing lesion in right middle cerebellar peduncle (*arrow*).**

***D*, T2-weighted axial image. Small area of increased intensity indicates presence of granulomatous lesion (*arrow*). Note absence of vasogenic edema.**

intimately to the neuroparenchyma and is detached from the arachnoid.

Capillary endothelial cells of the arachnoid have tight junctions, as do those in the brain, creating a CSF-blood barrier [19]. The basement membrane of the pia and adherent astrocytic foot processes creates a pial-brain barrier. In an animal model of meningeal carcinomatosis, Frank et al. [20] have shown that gadolinium not only enhances the infiltrated meninges but leaks into the contiguous CSF. Disruption of the capillary endothelial tight junctions of the arachnoid mater by disease most likely accounts for the passage of gadolinium into the adjacent pia mater and subarachnoid space [21].

Penetrating cerebral vessels are invested in a leptomeningeal sheath with a potential space continuous with subarachnoid space (the Virchow-Robin space) [16]. The first effect of leptomeningitis is meningeal vascular hyperemia. The ensuing inflammatory exudate spreads in the subarachnoid space and into the Virchow-Robin spaces to a variable degree. Infiltration may occur along the surface of the brain or extend deep into the brain along the Virchow-Robin spaces. The infiltrating process may appear intraparenchymal on gross examination or on MR images, but histologically the disease may remain restricted to the leptomeninges. A meningoencephalovasculopathy occurs when the pial-brain barriers are invaded by the inflammatory process [20].

Although we do not have direct pathologic correlation, progressive severity of the breakdown in the pial barriers can be inferred by noting the thickness of the pial enhancement, particularly along the brainstem. We speculate that if pial enhancement is seen as a sharply defined fine line there is disruption of the barriers, but probably no infiltration along perivascular spaces into the brain (Fig. 1). If the pial enhancement is thick and ragged (Fig. 4), then invasion along perivascular spaces has probably occurred, causing a meningoencephalovasculopathy, as has been shown on contrast-enhanced CT with pathologic correlation [16]. Enhancing

linear and nodular areas extending from the pial surface into the white matter indicate infiltration along Virchow-Robin spaces (Figs. 3 and 4).

Inflammation originating in the Virchow-Robin space can spread and coalesce, in the case of sarcoidosis, into granulomatous masses (Figs. 5 and 7). When this occurs there is often adjacent edema due to disruption of the blood-brain barrier and increased vascular permeability that extends along white matter fascicles (vasogenic edema) [22–24]. However, areas of blood-brain barrier disruption may be present without associated edema (Fig. 7). Vasogenic edema should be differentiated from chronic ischemic gliosis secondary to vasculopathy and perforating vessel occlusion caused by infiltration of Virchow-Robin spaces [16].

Dural involvement, although less frequent, is more likely than leptomeningeal disease to be detected on unenhanced MR. As noted previously [4], the only manifestations of CNS sarcoidosis on unenhanced MR images may be subtle falcine thickening or focal plaque formation. We have seen meningeal sarcoid produce a mass over the convexity [4], in the middle cranial fossa, and in the cerebellopontine angle. The varied appearances of CNS sarcoidosis on unenhanced MR are reviewed in Table 3. Typically there is intense enhancement in the abnormal area if gadopentetate dimeglumine is administered (Fig. 5). Falcine disease may develop as a consequence of local leptomeningeal granulomatous inflammation.

Sze et al. [13] anecdotally reported one patient with CNS sarcoidosis in whom the most striking abnormality was diffuse dural enhancement with minimal leptomeningeal enhancement.

Any portion of the brain can be affected by sarcoidosis, but the basal portion is the most common location [2, 25]. This correlates with recent observations that CSF-filled Virchow-Robin spaces are routinely visualized in the basal areas of the brain [26, 27]. Anatomically this area includes the anterior perforated substance, which is characterized by numerous penetrating, small blood vessels [28]. In addition, the blood-brain barrier is absent in the tuber cinereum, hypophysis, and preoptic region [24].

Hypothalamic dysfunction is the most common manifestation of CNS parenchymatous disease in sarcoidosis [1]. Seven of our patients had disease of the hypothalamic-pituitary axis (Figs. 1, 3, and 6). Pituitary infiltration by sarcoidosis is often reported histologically in patients with systemic sarcoidosis, but we are unaware of any report in the imaging literature [2, 29]. Optic chiasm and infundibular "thickening" are other common manifestations of CNS sarcoidosis on MR. The optic chiasm is enveloped by pia mater and therefore is subject to granulomatous leptomeningitis. Thickening of the chiasmatic pia as well as infiltration of the optic pathway can cause enlargement of the chiasm.

Seven of our patients had diffuse or focal areas of increased intensity in the periventricular white matter on T2-weighted images (Figs. 6 and 7). In two patients, periventricular white matter disease was detected only on T2-weighted images. Periventricular white matter lesions in CNS sarcoidosis have been reported previously [4, 8, 30]. In two patients the periventricular white matter disease resembled the common pattern of multiple sclerosis [31, 32]; in three patients the pattern was more typical of ischemic disease [33, 34]. In two patients probable mild interstitial edema was associated with hydrocephalus. One patient had extensive bilateral cerebellar gliosis or white matter infarctions that were hyperintense on T2-weighted images. The typical pattern of vasogenic edema was not seen and there was only mild meningeal enhancement around the cerebellum after administration of gadopentetate dimeglumine.

Hydrocephalus is a common manifestation of CNS sarcoidosis [1–3]. Granulomatous leptomeningitis may cause extraventricular obstructive hydrocephalus (communicating hydrocephalus) [6] or fourth ventricular outlet obstruction [18, 35]. Granulomatous compression of the aqueduct [16] and fourth ventricle [18] also may occur. Infiltration of the ependyma and choroid plexus may alter CSF dynamics resulting in hydrocephalus [2, 18]. Ependymal enhancement and prominent enhancement of the choroid plexus at the foramina of Luschka was seen in one of our patients (case 8).

There are several possible explanations for normal gadopentetate-dimeglumine–enhanced MR studies in our three patients with cranial nerve involvement. There may be extracranial involvement of the cranial nerves. There may be focal leptomeningeal or endoneurial disease that is too small to visualize or does not disrupt the blood-brain and pial barriers [2]. For example, some patients with aseptic and bacterial meningitis have normal gadopentetate-dimeglumine MR studies even if extraventricular obstructive hydrocephalus is present [11, 36]. Studies of carcinomatous meningitis have suggested that a minimum amount of tumor is required before enhancement is observed in the meninges on the enhanced images [13, 20]. There may have been reestablishment of the CSF-pial-brain barrier, thus preventing contrast enhancement despite the presence of active meningeal disease [20, 36]. We observed one patient in whom abnormal periventricular enhancement resolved after 6 months of therapy (Fig. 6).

The differential diagnosis of CNS sarcoidosis is quite broad. None of the unenhanced MR or gadopentetate-dimeglumine–enhanced manifestations of sarcoidosis are specific. Tuberculosis [37], fungal diseases, and bacterial [11, 36, 38] infections can produce diffuse leptomeningitis that may enhance on gadopentetate-dimeglumine MR. Meningeal carcinomatosis, leukemia, and lymphoma are indistinguishable from CNS sarcoidosis on MR [13]. We have seen diffuse meningeal enhancement following subarachnoid and subdural hemorrhage. Diffuse dural fibrosis following ventricular shunting has been shown to enhance intensely, but leptomeningeal involvement has been absent [39]. Less common diseases that could be diagnostic considerations in some cases include meningiomatosis [40], lipogranulomatosis [41], and cranial pachymeningitis [42].

Summary

1. It is important to understand that CNS sarcoidosis is foremost a leptomeningeal disease and the Virchow-Robin spaces are extensions of the leptomeninges. Study of gadopentetate-dimeglumine–enhanced images of the brain has solidified this concept.

2. We recommend the use of gadopentetate dimeglumine in all patients being evaluated for CNS sarcoidosis. Unenhanced MR alone is unlikely to reveal the important leptomeningeal manifestations of this disease.

3. Normal unenhanced and gadopentetate-dimeglumine–enhanced MR does not exclude CNS sarcoidosis, especially in patients with only cranial neuropathy or in those patients being treated with corticosteroids.

4. Enhancement with gadopentetate dimeglumine can resolve with corticosteroid treatment.

ACKNOWLEDGMENTS

We thank Stephen Reich, John Griffin, Claudio Levin, Penelope Scott, Gary Cassel, Justin McArthur, Thomas Price, Thomas Kowalski, Barbara Joslow, Philip Pulaski, Ben Frishberg, Andy Barbash, Robert Baumgartner, Sharon Seltzer, Patricia Behlmer, and Don Wood for patient referrals and Andrea Zanin and Shirley Zabrek for organizational and administrative assistance.

REFERENCES

1. Stern BJ, Krumholz A, Johns C, Scott P, Nissim J. Sarcoidosis and its neurological manifestations. *Arch Neurol* **1985**;42:909–917
2. Delaney P. Neurologic manifestations of sarcoidosis. *Ann Intern Med* **1977**;87:336–345
3. Ricker W, Clark M. Sarcoidosis: a clinical pathologic review of 300 cases, including 22 autopsies. *Am J Clin Pathol* **1949**;19:725–749
4. Hayes WS, Sherman JL, Stern BJ, Citrin CM, Pulaski PD. MR and CT evaluations of intracranial sarcoidosis. *AJNR* **1987**;8:841–847, *AJR* **1987**;149:1043–1049
5. Ketonen L, Oksanen V, Kuuliala I. Preliminary experience of magnetic resonance imaging in neurosarcoidosis. *Neuroradiology* **1987**;29:127–129
6. Miller DH, Kendall BT, Barter S, et al. Magnetic resonance imaging in central nervous system sarcoidosis. *Neurology* **1988**;38:378–383
7. Martin N, Debroucker T, Mompoint D, et al. Sarcoidosis of the pineal region: CT and MR studies. *J Comput Assist Tomogr* **1989**;13:110–112
8. Smith AS, Meisler DM, Weinstein MA, et al. High-signal periventricular lesions in patients with sarcoidosis: neurosarcoidosis or multiple sclerosis? *AJNR* **1989**;10:485–490
9. Berry I, Brant-Zawadzki M, Osaki L, Brasch R, Murovic J, Norman D. Gd-DTPA in clinical MR of the brain. 2. Extraaxial lesions and normal structures. *AJR* **1986**;147:1231–1235
10. Hesselink JR, Healy ME, Press GA, Brahme FJ. Benefits of Gd-DTPA for MR imaging of intracranial abnormalities. *J Comput Assist Tomogr* **1988**;12:266–274
11. Mathews VP, Kuharik MA, Edwards MK, D'Amour PG, Azzarelli B, Dreesen RG. Gd-DTPA–enhanced MR imaging of experimental bacterial meningitis: evaluation and comparison with CT. *AJNR* **1988**;9:1045–1050
12. Runge VM, Schaible TF, Goldstein HA, et al. Gd-DTPA clinical efficacy. *RadioGraphics* **1988**;8:147–159
13. Sze G, Soletsky S, Bronen R, Krol G. MR imaging of the cranial meninges with emphasis on contrast enhancement and meningeal carcinomatosis. *AJNR* **1989**;10:965–975
14. Delaney P. Neurologic manifestations in sarcoidosis. Review of the literature, with a report of 23 cases. *Ann Intern Med* **1977**;87:336–345
15. Osenbach RK, Blumenkopf B, Ramirez H, Gutierrez J. Meningeal neurosarcoidosis mimicking convexity en-plaque meningioma. *Surg Neurol* **1986**;26:387–390
16. Mirfakhraee M, Crofford MJ, Guinto FC, Nauta HJ, Weedn VW. Virchow-Robin space: a path of spread in neurosarcoidosis. *Radiology* **1986**;158:715–720
17. Kumpe DA, Rao CVGK, Garcia JH, et al. Intracranial neurosarcoidosis. *J Comput Assist Tomogr* **1979**;3:324–330
18. Schlitt M, Duvall ER, Bonnin J, Morawetz RB. Neurosarcoidosis causing ventricular loculation, hydrocephalus and death. *Surg Neurol* **1986**;26:67–71
19. Dyer ML, Parker JC. The meninges and their reactions to injury. In: Davis RL, Robertson DM, eds. *Textbook of neuropathology*. Baltimore: Williams & Wilkins, **1985**:138–146
20. Frank JA, Girton M, Dwyer AJ, Wright DC, Cohen PJ, Doppman JL. Meningeal carcinomatosis in the VX2 rabbit tumor model: detection with Gd-DTPA–enhanced MR imaging. *Radiology* **1988**;167:825–829
21. Ushio Y, Shimizu K, Aragaki Y, Arita N, Hayakawa T, Mogami H. Alteration of blood-CSF barrier by tumor invasion into the meninges. *J Neurosurg* **1981**;55:445–449
22. Klatzo I. Neuropathological aspects of brain edema. *J Neuropathol Exp Neurol* **1967**;26:1–11
23. Klatzo I, Suzuki R, Orzi R, Schuier F, Nitsch C. Pathomechanisms of ischemic brain edema. In: *Proceedings of the fifth international symposium on brain edema. Gronningen, the Netherlands 1982*. New York: Plenum, **1984**:1–10
24. Sage MR. Blood-brain barrier: phenomenon of increasing importance to the imaging clinician. *AJR* **1982**;138:887–898
25. Clark WC, Acker JD, Dohan FC, Robertson JH. Presentation of central nervous system sarcoidosis as intracranial tumors. *J Neurosurg* **1985**;63:851–856
26. Heier LA, Bauer CJ, Schwartz L, Zimmerman RD, Morgello S, Deck MDF. Large Virchow-Robin spaces: MR-clinical correlation. *AJNR* **1989**;10:929–936
27. Jungreis CA, Kanal E, Hirsch WL, Martinez AJ, Moosey J. Normal perivascular spaces mimicking lacunar infarction: MR imaging. *Radiology* **1988**;169:101–104
28. Crosby EC, Humphrey T, Lauer EW. *Correlative anatomy of the nervous system*. New York: Macmillan, **1962**:412–433
29. Bleisch VR, Robbins SL. Sarcoid-like granulomata of the pituitary gland. *Arch Intern Med* **1952**;89:877–892
30. Miller DH, Kendall BE, Barter S, et al. Magnetic resonance imaging in central nervous system sarcoidosis. *Neurology* **1988**;38:378–383
31. Horowitz AL, Kaplan RD, Grewe G, White RT, Salbert LM. The ovoid lesion: a new MR observation in patients with multiple sclerosis. *AJNR* **1989**;10:303–305
32. Uhlenbrock D, Seidel D, Gehlen W, et al. MR imaging in multiple sclerosis: comparison with clinical, CSF, and visual evoked potential findings. *AJNR* **1988**;9:59–67
33. Awad IA, Spetzler RF, Hodak JA, et al. Incidental subcortical lesions identified on magnetic resonance imaging in the elderly. I. Correlation with age and cerebrovascular risk factors. *Stroke* **1986**;162:509–511
34. Awad IA, Johnson PD, Spetzler RF, et al. Incidental subcortical lesions identified on magnetic resonance imaging in the elderly. II. Postmortem pathological correlations. *Stroke* **1986**;17:1090–1097
35. Lukin RR, Chambers AA, Soleimanpour M. Outlet obstruction of the fourth ventricle in sarcoidosis. *Neuroradiology* **1975**;10:65–68
36. Matthews VP, Smith RR, Bognanno JR, Kuharik MA, Edwards MK, Harris TM. Gd-DTPA enhanced MRI of meningitis; initial clinical experience (abstr). *AJNR* **1989**;10:1020
37. Suss RA, Resta S, Diehl JT. Persistent cortical enhancement in tuberculous meningitis. *AJNR* **1987**;8:716–720
38. Brown E, DeLaPaz R. Enhancement of meningeal lesions with gadopentetate (Gd-DTPA) MRI (abstr). *AJNR* **1989**;10:877
39. Destian S, Heier LA, Zimmerman RD, Morgello S, Deck MDF. Differentiation between meningeal fibrosis and chronic subdural hematoma after ventricular shunting: value of enhanced CT and MR scans. *AJNR* **1989**;10:1021–1026
40. Aoki S, Barkovich AJ, Nishimura K, et al. Neurofibromatosis types 1 and 2: cranial MR findings. *Radiology* **1989**;172:527–534
41. Tien RD, Brasch RC, Jackson DE, Dillon WP. Cerebral Erdheim-Chester disease: persistent enhancement with Gd-DTPA on MR images. *Radiology* **1989**;172:791–792
42. Martin N, Masson C, Henin D, Mompoint D, Marsault C, Nahum H. Hypertrophic cranial pachymeningitis: assessment with CT and MR imaging. *AJNR* **1989**;10:477–484